

Exploring Microphase Separation Behavior of Epoxidized Poly(styrene-*b*-isoprene-*b*-styrene) Block Copolymer Inside Thin Epoxy Coatings

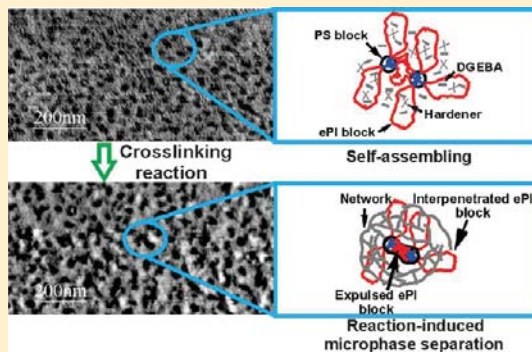
Hernan Garate,^{†,‡} Iñaki Mondragon,[§] Norma B. D'Accorso,^{†,*} and Silvia Goyanes^{‡,*}

[†]CIHIDECAR-CONICET, Departamento de Química Orgánica, FCEyN-UBA, Ciudad Universitaria 1428, Ciudad Autónoma de Buenos Aires, Argentina

[‡]IFIBA-CONICET; LP&MC, Departamento de Física, FCEyN-UBA, Ciudad Universitaria 1428, Ciudad Autónoma de Buenos Aires, Argentina

[§]Departamento de Ingeniería Química y Medio Ambiente, Escuela Politécnica, University of the Basque Country, Pza. Europa 1, 20018 Donostia-San Sebastián, Spain

ABSTRACT: We report an investigation of the mechanisms involved in the formation of nanostructured epoxy thermosetting systems using highly epoxidized poly(styrene-*b*-isoprene-*b*-styrene) (eSIS) block copolymer at three different stages of the curing process. In the uncured state, polystyrene (PS) blocks self-assembled in sphere-like nanodomains with a short-range order, while epoxidized polyisoprene (ePI) subchains were initially miscible with the epoxy precursors. As the curing reaction proceeded, the PS nanodomains became gradually distorted switching to bigger and less organized structures. This effect is due to reaction-induced microphase separation of ePI subchains which became immiscible with the epoxy system as the curing process occurs. However, this demixing process was partial because of the reaction between ePI subchains and the epoxy matrix, which reduced ePI subchains mobility. Non expelled ePI fraction increased the epoxy matrix mean glass transition temperature (T_g) in (20–25) °C. Moreover, it was demonstrated that the epoxidation degree of ePI subchains affected the final obtained nanostructured pattern of the thermosetting materials, switching from distorted and interconnected sphere-like nanodomains when the epoxidation degree is 65% to sphere-like nanostructures for 100% of epoxidation.



INTRODUCTION

The use of block copolymers for the development of nanostructured epoxy thermosetting systems has attracted great attention in recent years. By forming ordered (or disordered) nanostructures inside thermosets the properties of materials can be further optimized.^{1–5} Many efforts have been devoted to understand the formation mechanisms of nanostructures in epoxy thermosets, which is crucial for controlling the morphology of the obtained nanosized elements. Depending on the solubility of the different block copolymer subchains, self-assembly can be obtained before curing, if only one block is selectively miscible with epoxy precursors,^{5–9} or during the curing reaction, if all subchains of the block copolymer are initially miscible with the epoxy precursors but one of them undergoes phase-separation as the polymerization reaction proceeds due to increasing immiscibility with the thermosetting matrix.^{10–12}

The most common epoxy miscible blocks used for this purpose have been poly(ethylene oxide), polycaprolactone and poly(methyl methacrylate).^{13–16} These blocks are miscible with the epoxy matrix by forming intermolecular hydrogen bonding after curing. The main disadvantage of this strategy is that the

interpenetrated nonreactive blocks act as plasticizers reducing the T_g values of the thermoset.^{17,18}

In order to overcome this issue, different block copolymers with reactive groups in the miscible block have been designed. Chemically bonding the block copolymer to the resin can also fix the developed nanostructures inside the matrix. In this regard, styrenic block copolymers such as poly(styrene-*b*-butadiene-*b*-styrene) or poly(styrene-*b*-isoprene-*b*-styrene) (SIS) are the most widely used thermoplastic elastomers. They present styrenic subchains as hard block and a polybutadiene or polyisoprene subchain as soft block. The use of such block copolymers as templates for nanostructured thermosets is of great interest since they are commercially available at considerable low costs, which is an important aspect for potential applications. For this purpose, the epoxidation of polybutadiene block of poly(styrene-*b*-butadiene-*b*-styrene) block copolymer or polyisoprene block of SIS block copolymer emerged as an excellent strategy to make them miscible with

Received: January 3, 2013

Revised: March 5, 2013

Published: March 15, 2013



the epoxy precursors.^{19,20} Moreover, by this chemical modification the obtained block copolymers can react with the epoxy system during curing fixing the nanostructures inside the matrix. In this field, Mondragon and co-workers have extensively investigated the use of epoxidized polybutadiene as a reactive block of a poly(styrene-*b*-butadiene-*b*-styrene) block copolymer,^{21,22} whereas Bates and col. investigated epoxidized polyisoprene (ePI) block as a reactive block of a poly-(butadiene-*b*-isoprene) diblock copolymer.²³

Because of the fact that high epoxidation degrees are necessary to ensure miscibility of the ePI blocks with the resin, we have recently described a methodology to epoxidize SIS block copolymers minimizing typical undesirable side-products and showed that highly epoxidized SIS block copolymer serve as templates for nanostructured thermosets.²⁴ However, the question of how the final ordered/disordered state is achieved was not fully explored previously in the literature. Previous works generally explained the formation of nanostructures by self-assembly or by reaction-induced microphase separation without considering the final morphologies as a result of a combination of both processes. In this regard, Bates and co-workers²⁵ studied the formation of nanostructured thermosets using a poly(ethylene oxide)–poly(ethyl ethylene) nonreactive block copolymer, and found that once an ordered state has been prepared by self-assembly, the cross-linking of the epoxy resin does not affect the final morphology since both processes are uncoupled. However, this is not the case for a reactive block copolymer such as eSIS. In such system, self-assembly and polymerization are coupled since block copolymer can also participate in the curing process affecting the final morphology.

Therefore, the purpose of this work is twofold: to study the morphological evolution developed by eSIS block copolymers inside thermosets at different stages of the curing process in order to propose a possible nanostructuration mechanism, and to evaluate how the epoxidation degree affects the obtained nanostructured pattern.

EXPERIMENTAL SECTION

Materials. A commercial cylinder forming²⁶ poly(styrene-*b*-isoprene-*b*-styrene) (SIS) block copolymer Kraton SIS-D1165 was epoxidized using the previously reported strategy²⁴ in three different epoxidation degrees: 65% (SIS65), 85% (SIS85) and 100% (SIS100). The epoxy monomer, diglycidyl ether of bisphenol A (DGEBA), Epikote 828, was purchased from Hexion. It has an epoxy equivalent of around 184–190. The hardener was a mixture of amines under the commercial name of Ancamine 2500 (1-(2-aminoethyl)piperazine:1,3-bis(aminomethyl)benzene; 1:2 mol/mol), supplied by Air Products. The chemical formulas of all the epoxy components used for this study are given in Figure 1.

Preparation of Epoxy Thermosets Containing Block Copolymers. Films with an eSIS content of 23 wt % were prepared as follows. Epoxidized SIS was dissolved in toluene and sonicated for 30 min. DGEBA was added to the solution and sonicated for further 30 min. Ancamine was then added to the resulting solution. The used epoxy/amine ratios between each component were those that provided the maximum T_g value: DGEBA (1 equiv), eSIS (0.5 equiv for SIS65; 0.6 equiv for SIS85; 0.7 equiv for SIS100), ancamine (1.3 equiv). After sonication for 5 min, the solutions were drop-cast on a silicon substrate, previously cleaned with acetone and ethanol, and finally dried in high purity nitrogen. The solvent was evaporated at room temperature for 12 h (*stage one*) and then the films were cured at 80 °C for 100 min (*stage two*) or 180 min (*stage three*) under vacuum. The obtained films had a thickness of $(7 \pm 1) \mu\text{m}$ as determined by digital micrometer.

For isothermal DSC experiments, samples were prepared differently in order to avoid measuring the endothermic process associated with

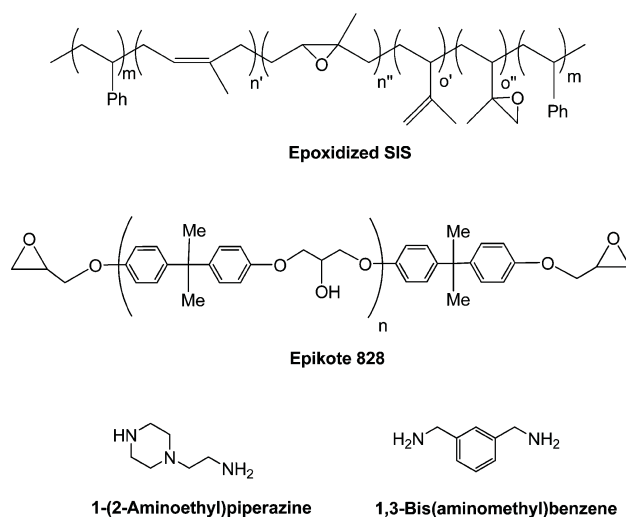


Figure 1. Epoxy components used in this study.

solvent evaporation: eSIS was dissolved in tetrahydrofuran and sonicated for 30 min. DGEBA was added to the solution and sonicated for further 30 min. Then the solvent was evaporated under vacuum. Ancamine was then added to the mixture with vigorous stirring until a homogeneous sample was obtained and immediately measured by DSC.

Differential Scanning Calorimetry (DSC). Calorimetric measurements were made on a TA Q20 differential scanning calorimeter in a dry nitrogen atmosphere. Indium standard was used for calibration. Samples of 5–10 mg were placed in the DSC pan. For dynamic experiments the samples used were the same than those prepared for AFM measurement. The films were detached from the silicon wafer prior to the DSC scans. Samples were first heated to 150 °C and held at that temperature for 10 min to remove the thermal history. Then, samples were cooled to –80 °C at a rate of 20 °C/min, held for 10 min, and again heated to 150 °C at 20 °C/min. The T_g values were taken as the midpoint of the transition in the second heating scan. For isothermal experiments, samples were equilibrated at a certain temperature and held for the corresponding time of the experiment. Two experimental conditions were used in this work for the isothermal DSC measurements: 20 °C for 12 h, which is required for solvent evaporation, and 80 °C for 180 min, which is required for curing the epoxy resin as previously reported.²⁴

Fourier Transform Infrared Spectroscopy (FTIR). The FTIR spectra of all samples were measured with a Nicolet 510 P equipment using the KBr disk method. Samples were mixed with the KBr powder and ground well, and then KBr disks were prepared. The spectra were recorded by the average of 32 scans in the standard wavenumber range of 4000–400 cm^{-1} . The baseline was corrected and normalized to the 1035 cm^{-1} peak height corresponding to the DGEBA aliphatic ether linkage.²⁷

Atomic Force Microscopy (AFM). The morphology features of the nanostructured epoxy thermosetting films were investigated by AFM. AFM images were obtained operating in the soft tapping mode with a scanning probe microscope (Nanoscope IIIa, Multimode from Digital Instruments).

RESULTS AND DISCUSSION

Microphase Separation Behavior. The successful preparation of nanostructured epoxy thermosets containing 23 wt % of SIS85 was described in our previous work.²⁴ In order to determine the mechanisms by which microphase separation occurs in such systems, the morphology of transparent film composites was studied by AFM at three different stages of the curing process: (1) before curing (*stage one*); (2) after curing at 80 °C for 100 min (*stage two*); (3) after curing at 80 °C for 180

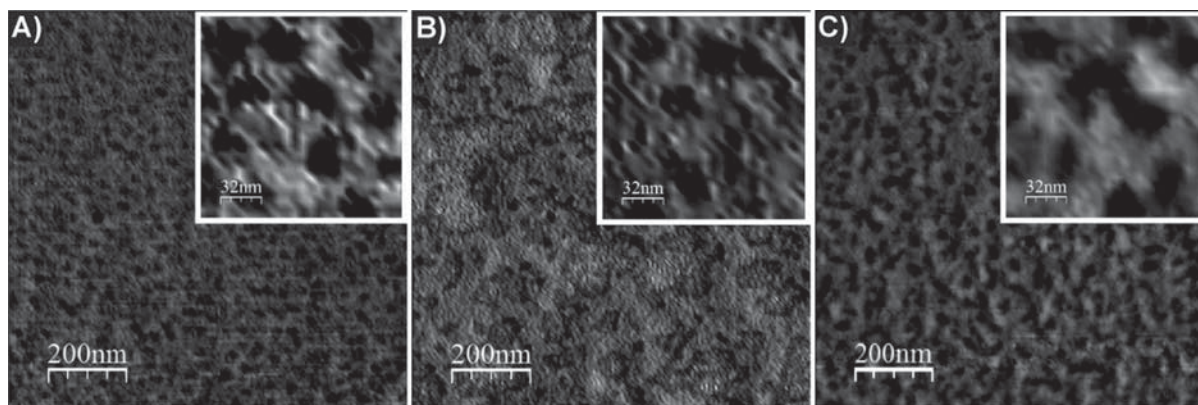


Figure 2. Tapping mode-AFM phase image of epoxy system/SIS85 (23 wt %) blends for (a) stage one, (b) stage two, and (c) stage three.

min (stage three). Figure 2a shows AFM phase images for composite at stage one, where sphere-like nanostructures well dispersed in the matrix can be observed. At stage two less ordered sphere-like nanostructures were obtained, as shown in Figure 2b. The nanodomains switched to bigger and less organized structures at stage three, as observed in Figure 2c.

The obtained nanostructures at stage one are likely due to self-assembling of PS subchains, which are not miscible with the epoxy precursors.

When the samples were cured for 100 min at 80 °C (stage two), some interconnected PS nanodomains appeared, although the size of the spherical nanostructures remained almost invariant. Stage three samples presented a completely different morphology. Distorted sphere-like nanophases were found with bigger size and much less organized than for previous stages. This gradual morphological evolution of the system strongly suggest that phase separation also develops as cross-linking proceeds, based on the principles of the reaction-induced microphase separation mechanism leading to bigger and less organized nanostructures. Although the ePI subchains are initially miscible with the epoxy precursors, immiscibility increases as the curing reaction proceeds. The ePI block demixing leads to a broadening and loss of regularity in the obtained nanodomains.

Therefore, the initially obtained nanostructure is due to mixing. Moreover, when the system is cured, the morphology is affected switching to distorted sphere-like nanodomains. This temporal evolution is due to partial expulsion of ePI block.

Reactivity. In a previous work we demonstrated by means of dynamic DSC experiments the ability of SIS85 to react with the hardener during the curing process.²⁴ In order to determine the reaction extent of SIS85/DGEBA/hardener at stage one, isothermic DSC at 20 °C was performed for 12 h showing an exothermic process beginning from 5 h. From the isothermic DSC experiments for SIS85/DGEBA/hardener at 80 °C shown in Figure 3 it was evidenced that at stage three the curing process was already ended, and therefore it was considered as the maximum conversion. By comparing the normalized area under the isothermic DSC curves for SIS85/DGEBA/hardener at stage one and stage three the reaction extent during stage one was calculated to be 2%. Even though this calculation is for samples that were solvent evaporated prior to hardener addition, a similar low reaction extent is expected for those samples which were not treated under vacuum before the hardener was added. Therefore, the obtained nanostructure at stage one is due to self-assembling of PS subchains. By applying

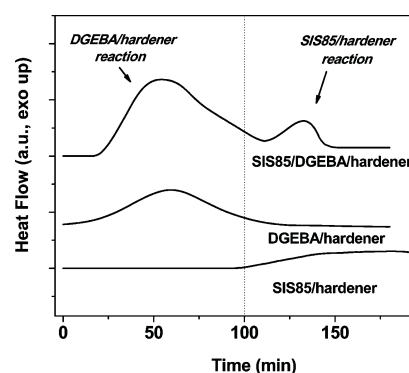


Figure 3. Isothermic DSC at 80 °C during 180 min for SIS85/DGEBA/hardener; DGEBA/hardener; SIS85/hardener.

a similar procedure, the reaction extent for stage two was calculated to be 92%.

To prove the ability of the ePI subchains to react with the epoxy system, isothermic DSC experiments at 80 °C were performed as shown in Figure 3. DGEBA/hardener system presented an exotherm with t_{\max} at 60 min corresponding to the curing process. On the other hand, SIS85/hardener system possessed an exothermic peak starting at 100 min when DGEBA/hardener was almost reacted. Between stage two and stage three (from 100 to 180 min) both DGEBA and SIS85 were able to react simultaneously with the hardener. From the DSC curves it was evidenced that reaction between DGEBA/hardener was faster than that for SIS85/hardener, which is in agreement with previous work.²³ Therefore, it was anticipated that if expelled the ePI subchains could react with the hardener leading to an ePI rich phase. On the contrary, if ePI chains were not expelled during curing it was expected that they could cross-link with the epoxy system during the final curing stage.

From the heat evolved for DGEBA/hardener, DGEBA/SIS85/hardener, and SIS85/hardener presented in Table 1, ΔH values were calculated to be in the range of about 100 kJ/mol epoxy. These values are in good agreement with those for many amine/epoxy condensation systems, which are generally in the range of 100 kJ/mol.²⁸

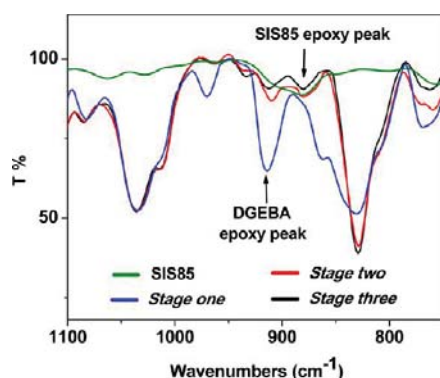
It is worth noting that these values differ from that calculated by de Bakker et al. (65 kJ/mol epoxy)²⁹ for a system where a tertiary amine initiates the homopolymerization/etherification side reaction which competes with the epoxy/amine con-

Table 1. Heat of Reaction for DGEBA/Hardener, DGEBA/SIS85/Hardener, and SIS85/Hardener Calculated from DSC Experiments

	$\Delta H(\text{kJ/mol})$
DGEBA/hardener	98 ± 5
DGEBA/SIS85/hardener	95 ± 5
SIS85/hardener	96 ± 5
epoxy/amine condensation ²⁸	100 ± 5
epoxy/amine condensation + etherification ²⁹	65 ± 5

densation reaction. Therefore, in the current system the main occurring reaction is the epoxy/amine condensation.

The reaction process was also investigated by FTIR spectroscopy, as shown in Figure 4. Among the many peaks

**Figure 4.** FTIR spectra showing the curing behavior of epoxy system/SIS85 (23 wt %) blends for stage one (blue), stage two (red), stage three (black), and SIS85 (green).

the most important peaks are the one at 912 cm^{-1} , which corresponds to the asymmetric stretching absorption of DGEBA oxirane ring,³⁰ and the less intense epoxy signal of the ePI block at 880 cm^{-1} ,²⁴ which appears as a broad peak due to the presence of an oxirane ring from both 1,4- and 3,4-addition of the isoprene repeat unit of polyisoprene. By following the relative intensity of both peaks, the evolution of the curing process can be studied for the three different stages.

The 912 cm^{-1} peak was substantially decreased between stage one and stage two as the reaction DGEBA/hardener progressed, while the broad ePI epoxy peak at 880 cm^{-1} remained unchanged since no reaction between ePI subchains and the

hardener occurs during that stage. Interestingly the ePI epoxy signal at 880 cm^{-1} was slightly reduced at stage three, giving evidence of the reaction between ePI blocks and the hardener. The signal at 912 cm^{-1} almost disappears at stage three, indicating that only residual epoxy groups remained unreacted.

Effect of the Epoxidation Degree. Because of the fact that the miscibility of ePI subchains with the epoxy precursors depends on the ePI epoxidation degree, it was expected that lower epoxidation degrees would lead to higher amount of expulsion during the curing process and therefore differences on the morphology. For this purpose, the morphology of cured blends using SIS65, SIS85 and SIS100 were compared, as shown in Figure 5.

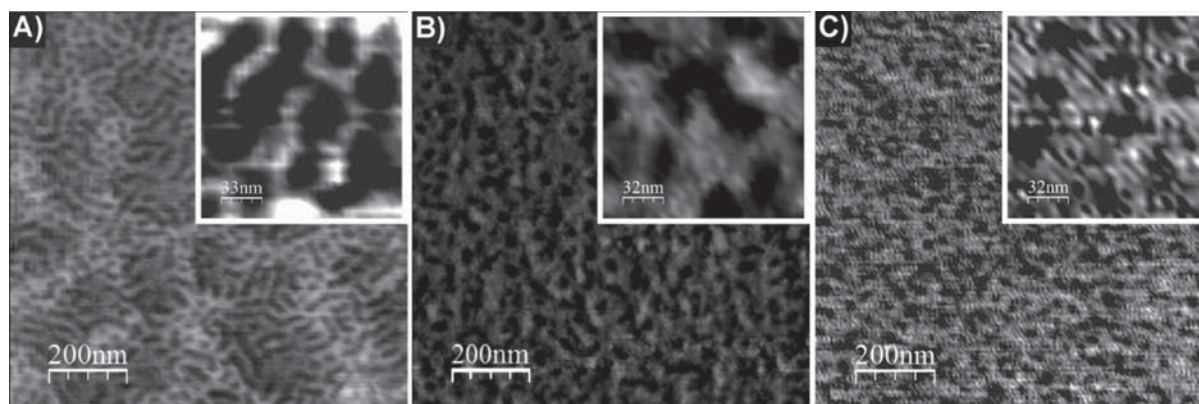
In all the cases, the epoxy thermosets containing eSIS were microphase-separated, and the morphologies were quite dependent on the epoxidation degree. The obtained nanostructures for epoxy system/SIS65 were a combination of sphere-like structures and interconnected spheres, as shown in the inset of Figure 5a. By increasing the epoxidation degree to 85%, it was observed that the obtained sphere-like structures were distorted and presented less interconnections than for the case of 65% (Figure 5b). For the higher epoxidation degree of 100%, the sphere-like nanodomains seem to be even less interconnected (Figure 5c).

The previous trend can be interpreted in terms of the initially miscible ePI block tendency to be demixed out of the epoxy matrix on the basis of the reaction-induced microphase separation mechanism. The higher the epoxidation degree is, the lower the demixing process is, and therefore less interconnected sphere-like structures were formed. Accordingly, a new ePI rich phase should be formed in the vicinity of the PS nanodomains, which was studied by DSC.

Dynamic DSC experiments showed that SIS block copolymer presented a major T_g at $-50\text{ }^{\circ}\text{C}$, which corresponds to the polyisoprene block, and a minor T_g at $85\text{ }^{\circ}\text{C}$ attributed to the PS blocks.²⁴

Figure 6 shows the DSC curves for eSIS, where it can be seen that ePI T_g shifts from -5 to $+23\text{ }^{\circ}\text{C}$ when the epoxidation degree increases from 65 to 100%, due to the increased rigidity introduced by oxiranic rings. Moreover, the increment of ePI T_g value for the different eSIS/hardener cured systems indicated the ability of the ePI blocks to react with the hardener.

The nanostructured epoxy thermosets possess interesting phase behavior since ePI block reacts with the hardener forming covalent bonding with epoxy networks. As can be

**Figure 5.** Tapping mode-AFM phase image of cured epoxy system/eSIS (23 wt %) blends for (a) SIS65, (b) SIS85, and (c) SIS100.

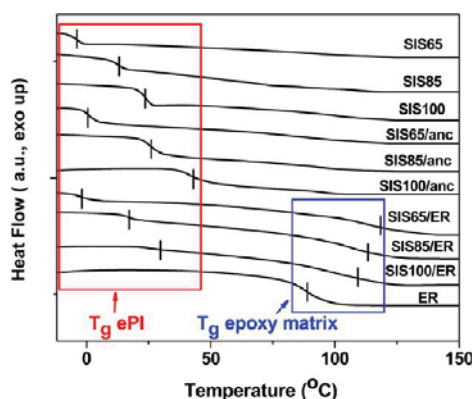


Figure 6. DSC curves of the second scan of eSIS, eSIS/hardener, and eSIS/ER cured blends.

observed in Figure 6, all cured epoxy systems with the different eSIS show two T_g values. It is worth noting that the used scale does not allow visualizing PS T_g , which is about 7 wt % in the thermosetting materials. However, this transition occurs at 85 °C and is coupled with DGEBA/hardener T_g .

The minor transition at lower temperatures corresponds to an ePI rich phase associated with the demixing behavior of ePI blocks in the process of reaction-induced microphase separation. It is worth noting that the ePI rich phase T_g value in all nanostructured thermosets was higher than that for each pure ePI block (Table 2), due to reaction between demixed ePI

Table 2. ePI T_g Values of eSIS, eSIS/ER, and eSIS/Hardener

	T_g (°C) 65%	T_g (°C) 85%	T_g (°C) 100%
eSIS	−5	12	23
eSIS/ER	−1	17	27
eSIS/hardener	1	26	42

blocks and the hardener. Moreover, the minor T_g value is lower than that observed for each eSIS cured with the hardener meaning that the ePI blocks in the nanostructured systems were partially reacted with the hardener, likely due to less flexibility in the thermosetting materials. The second transition observed at higher temperatures is attributed to the epoxy matrix rich phase. In comparison to the T_g of the DGEBA/hardener system (ER), this transition was broadened and the mean value was shifted to higher temperatures in (20–25) °C. In terms of the fact that the temperatures of the major transition was increased by the addition of eSIS, it is proposed

that interpenetrated ePI blocks were to some extent able to react with the hardener and cross-link with DGEBA during *stage three* of the curing reaction, modifying the structure of the epoxy matrix and filling the matrix free volume. Covalent bonds between interpenetrated ePI blocks and the epoxy matrix avoid the demixing process up to some extent.

A schematic illustration of the nanostructure behavior of eSIS inside the epoxy matrix is shown in Scheme 1. At an early stage of the curing process, where cross-linking reaction has not started (uncured state), PS subchains self-assemble in sphere like nanodomains (blue) due to their high immiscibility with the epoxy precursors. The soluble ePI blocks (red) form loops and bridges between condensed PS cores.³¹ In the cured state, less ordered and bigger nanostructures are obtained, likely due to interconnection of PS nanodomains. As the cross-linking reaction proceeds, ePI subchains became immiscible with the epoxy matrix and therefore expelled from the forming network. However, a non-negligible fraction of ePI subchains remain interpenetrated in the epoxy matrix increasing its T_g mean value, likely by filling free volume.

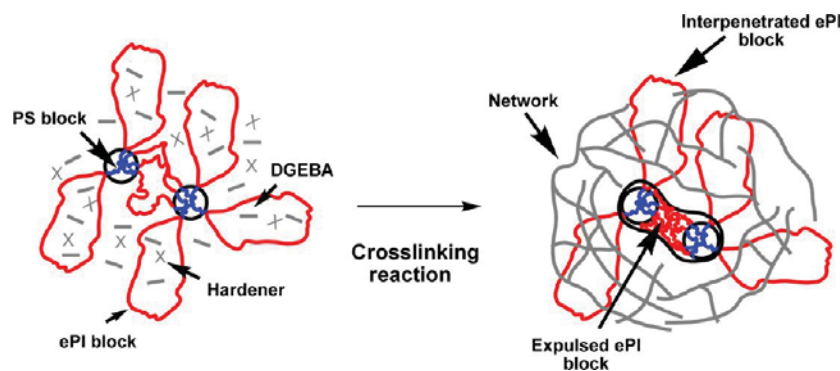
CONCLUSIONS

In this work, it was demonstrated that the development of nanostructures in thermosetting epoxy systems using highly epoxidized SIS block copolymer depends on two different mechanisms. A first self-assembling of PS subchains, which occurs at an early stage of the curing process, where the reaction extent was only 2%, as determined by DSC experiments. Self-assembling leads to sphere-like nanodomains with a short-range order, as observed by AFM.

As the curing process progressed, reaction-induced microphase separation of ePI subchains occurred leading to a gradual distortion of PS sphere-like nanostructures and the formation of an ePI rich phase, as evidenced by DSC. By increasing the epoxidation degree of ePI subchains, this effect was less pronounced due the higher miscibility of ePI blocks with the epoxy system. Moreover, ePI demixing process is partial because of its reduced mobility given by covalent bonds with the epoxy matrix and its high mean molecular weight. The ePI fraction that was not expelled from the epoxy matrix increased the epoxy matrix mean T_g value by 20–25 °C, likely by filling free volume.

These materials are of great interest for the development of novel reinforced nanostructured epoxy thermosets with applications in aeronautic industry.

Scheme 1. Uncured (Left) and Cured (Right) State for SIS85/DGEBA/Hardener



AUTHOR INFORMATION

Corresponding Author

*E-mail: (S.G.) sgoyanes@df.fcen.uba.ar; (N.B.D.) norma@qo.fcen.uba.ar.

Notes

The authors declare no competing financial interest.

ACKNOWLEDGMENTS

The authors express thanks for the financial support of UBACyT (Nos. 20020100100350 and 200220100100142), ANPCyT 200700291, and CONICET (PIP11220080100064 and PIP 11220090100699) and the fellowship of H.G. from Argentina. The authors are also thankful for funding from the European Community (POCO project, 7th FP, NMP-213939).

REFERENCES

- (1) Ruiz-Perez, L.; Royston, G. J.; Fairclough, P. A.; Ryan, A. J. *Polymer* **2008**, *49*, 4475–4488.
- (2) Liu, J.; Thompson, Z. J.; Sue, H.-J.; Bates, F. S.; Hillmyer, M. A.; Dettloff, M.; Jacob, G.; Verghese, N.; Pham, H. *Macromolecules* **2010**, *43*, 7238–7243.
- (3) Declet-Perez, C.; Redline, E. M.; Francis, L. F.; Bates, F. S. *ACS Macro Lett.* **2012**, *1*, 338–342.
- (4) Wu, S.; Guo, Q.; Peng, S.; Hameed, N.; Kraska, M.; Stühn, B.; Mai, Y.-W. *Macromolecules* **2012**, *45*, 3829–3840.
- (5) Mijovic, J.; Shen, M.; Sy, J. W.; Mondragon, I. *Macromolecules* **2000**, *33*, 5235–5244.
- (6) Ritzenthaler, S.; Court, F.; David, L.; Girard-Reydet, E.; Leibler, L.; Pascault, J. P. *Macromolecules* **2002**, *35*, 6245–6254.
- (7) Ritzenthaler, S.; Court, F.; Girard-Reydet, E.; Leibler, L.; Pascault, J. P. *Macromolecules* **2003**, *36*, 118–126.
- (8) Xu, Z.; Zheng, S. *Polymer* **2007**, *48*, 6134–6144.
- (9) Maiez-Tribut, S.; Pascault, J. P.; Soulé, E. R.; Borrajo, J.; Williams, R. J. J. *Macromolecules* **2007**, *40*, 1268–1273.
- (10) Meng, F.; Zheng, S.; Li, H.; Liang, Q.; Liu, T. *Macromolecules* **2006**, *39*, 5072–5080.
- (11) Yu, R.; Zheng, S. *Macromolecules* **2011**, *44*, 8546–8557.
- (12) Meng, F.; Xu, Z.; Zheng, S. *Macromolecules* **2008**, *41*, 1411–1420.
- (13) Zhu, L.; Zhang, C.; Han, J.; Zheng, S.; Li, X. *Soft Matter* **2012**, *8*, 7062–7072.
- (14) Yu, R.; Zheng, S.; Li, X.; Wang, J. *Macromolecules* **2012**, *45*, 9155–9168.
- (15) Rebizant, V.; Venet, A.-S.; Tournilhac, F.; Girard-Reydet, E.; Navarro, C.; Pascault, J. P.; Leibler, L. *Macromolecules* **2004**, *37*, 8017–8027.
- (16) Wu, S.; Peng, S.; Hameed, N.; Guo, Q.; Mai, Y.-W. *Soft Matter* **2012**, *8*, 688–698.
- (17) Apohama, N. K.; Yilmaza, O. K.; Baysalc, K.; Baysal, B. M. *Polymer* **2001**, *42*, 4109.
- (18) Videki, B.; Klebert, S.; Pukanszky, B. *J. Polym. Sci., Part B: Polym. Phys.* **2007**, *45*, 873.
- (19) Grubbs, R. B.; Broz, M. E.; Dean, J. M.; Bates, F. S. *Macromolecules* **2000**, *33*, 2308–2310.
- (20) Serrano, E.; Larrañaga, M.; Remiro, P. M.; Mondragon, I.; Carrasco, P. M.; Pomposo, J. A.; Mecerreyes, D. *Macromol. Chem. Phys.* **2004**, *205*, 987–996.
- (21) Serrano, E.; Tercjak, A.; Kortaberria, G.; Pomposo, J. A.; Mecerreyes, D.; Zafeiropoulos, N. E.; Stamm, M.; Mondragon, I. *Macromolecules* **2006**, *39*, 2254–2261.
- (22) Ramos, J. A.; Esposito, L. H.; Fernandez, R.; Zalakian, I.; Goyanes, S.; Avgeropoulos, A.; Zafeiropoulos, N. E.; Kortaberria, G.; Mondragon, I. *Macromolecules* **2012**, *45*, 1583–1591.
- (23) Grubbs, R. B.; Dean, J. M.; Broz, M. E.; Bates, F. S. *Macromolecules* **2000**, *33*, 9522–9534.
- (24) Garate, H.; Mondragon, I.; Goyanes, S.; D'Accorso, N. *J. Polym. Sci., Part A: Polym. Chem.* **2011**, *49*, 4505–4513.
- (25) Hillmyer, M. A.; Lipic, P. M.; Hajduk, D. A.; Almdal, K.; Bates, F. J. *Am. Chem. Soc.* **1997**, *119*, 2749–2750.
- (26) Garate, H.; Fascio, M.; Mondragon, I.; D'Accorso, N. B.; Goyanes, S. *Polymer* **2011**, *52*, 2214–2220.
- (27) Meure, S.; Wu, D.-Y.; Furman, S. A. *Vib. Spectrosc.* **2010**, *52*, 10–15.
- (28) Ooi, S. K.; Cook, W. D.; Simon, G. P.; Such, C. H. *Polymer* **2000**, *41*, 3639–3649.
- (29) De Bakker, C. J.; St John, N. A.; George, G. A. *Polymer* **1993**, *34*, 716–725.
- (30) Hameed, N.; Gou, Q.; Xu, Z.; Hanley, T. L.; Mai, Y.-W. *Soft Matter* **2010**, *6*, 6119–6129.
- (31) Zhulina, E. B.; Borisov, O. V. *Macromolecules* **2012**, *45*, 4429–4440.